Title

COOH-terminal truncated alpha(1S) subunits conduct current better than full-length dihydropyridine receptors.

Journal

The Journal of general physiology, 116(3)

ISSN

0022-1295

Authors

Morrill, JA
Cannon, SC

Publication Date

2000-09-01

DOI

10.1085/jgp.116.3.341

Peer reviewed

COOH-terminal Truncated Alpha$_{1S}$ Subunits Conduct Current Better than Full-length Dihydropyridine Receptors

James A. Morrill* and Stephen C. Cannon*‡

From the *Program in Neuroscience, Department of Neurobiology, Harvard Medical School, Boston, Massachusetts 02115; and ‡Department of Neurology, Massachusetts General Hospital, Boston, Massachusetts 02114

abstract Skeletal muscle dihydropyridine (DHP) receptors function both as voltage-activated Ca^{2+} channels and as voltage sensors for coupling membrane depolarization to release of Ca^{2+} from the sarcoplasmic reticulum. In skeletal muscle, the principal or α_{1S} subunit occurs in full-length (~10% of total) and post-transcriptionally truncated (~90%) forms, which has raised the possibility that the two functional roles are subserved by DHP receptors comprised of different sized α_{1S} subunits. We tested the functional properties of each form by injecting oocytes with cRNAs coding for full-length (α_{1S}) or truncated ($\alpha_{1S\Delta C}$) α subunits. Both translation products were expressed in the membrane, as evidenced by increases in the gating charge (Q_{max} 80–150 pC). Thus, oocytes provide a robust expression system for the study of gating charge movement in α_{1S}, unencumbered by contributions from other voltage-gated channels or the complexities of the transverse tubules. As in recordings from skeletal muscle, for heterologously expressed channels the peak inward Ba^{2+} currents were small relative to Q_{max}. The truncated $\alpha_{1S\Delta C}$ protein, however, supported much larger ionic currents than the full-length product. These data raise the possibility that DHP receptors containing the more abundant, truncated form of the α_{1S} subunit conduct the majority of the L-type Ca^{2+} current in skeletal muscle. Our data also suggest that the carboxyl terminus of the α_{1S} subunit modulates the coupling between charge movement and channel opening.

key words: Ca^{2+} channels • skeletal muscle • *Xenopus* oocyte expression • cut-open oocyte voltage clamp • gating charge movement

INTRODUCTION

Skeletal muscle dihydropyridine (DHP)[1] receptors are L-type Ca^{2+} channels that serve a dual role in muscle, functioning both as Ca^{2+}-conducting pores and as the voltage sensors for excitation–contraction (E-C) coupling (Ríos and Brum, 1987; Tanabe et al., 1988; Melzer et al., 1995). These channels are heteromeric complexes containing the pore-forming α_{1S} subunit plus the β_1, $\alpha_2\delta$, and γ regulatory subunits (Hofmann et al., 1994). Two forms of the α_{1S} subunit have been detected in skeletal muscle: a 212-kD full-length translation product (α_{1S}), present as a minor component, and a more abundant 175-kD form ($\alpha_{1S\Delta C}$, 90% of α_1 subunit recovered from transverse tubule membrane preparations) created by post-translational cleavage of 175 amino acids from the COOH terminus (De Jongh et al., 1989, 1991). While the COOH termini of other cloned Ca^{2+} channel α_1 subunits have been shown to play a role in channel regulation (Wei et al., 1994; Lee et al., 1999; Zühlke et al., 1999), the functional significance of the COOH-terminal truncation of α_{1S} is unknown.

One long-standing hypothesis holds that some DHP receptors in skeletal muscle are specialized voltage sensors for E-C coupling, while others are capable of both voltage sensing and Ca^{2+} conduction. Comparison of DHP binding to L-type Ca^{2+} current amplitude in intact muscle fibers suggested that only a small percentage of DHP receptors are functional Ca^{2+} channels (Schwartz et al., 1985). The discovery of two size forms of α_{1S} occurring in a 90%:10% ratio led to the hypothesis that the rarer full-length form is capable of both sensing the voltage and passing current, while the more abundant truncated form is a dedicated voltage sensor for E-C coupling (De Jongh et al., 1989).

Injection of cDNAs encoding either α_{1S} or a COOH-terminally truncated form of α_{1S} (at Asn 1662) into the nuclei of dysgenic mouse myotubes lacking α_{1S} restores contraction, gating charge movement, and L-type Ca^{2+} current (Tanabe et al., 1988; Adams et al., 1990; Beam et al., 1992). While the version of $\alpha_{1S\Delta C}$ used in these experiments was artificially truncated slightly upstream of the native cleavage site, these results clearly suggest that $\alpha_{1S\Delta C}$ can function as both an ion channel and a voltage sensor for E-C coupling. However, the role of full-length α_{1S} remains unknown, since it is possible that an undetermined proportion of the α_{1S} subunits were cleaved to $\alpha_{1S\Delta C}$ in the myotubes. One recent study has address this issue. When the green fluores-

Address correspondence to Stephen C. Cannon, M.D., Ph.D., EDR 413 / Massachusetts General Hospital, Fruit Street, Boston, MA 02114. Fax: 617-726-3926; E-mail: cannon@helix.mgh.harvard.edu

[1]*Abbreviations used in this paper:* DHP, dihydropyridine; E-C, excitation–contraction.

cent protein was fused to the COOH terminus of α_{1S} and expressed in dysgenic myotubes, the fluorescence was localized to the t tubules, which suggests a significant amount of full-length α_{1S} was inserted into the membrane and little cleavage occurred within the 48–72-h duration of the experiment (Flucher et al., 1999).

Heterologous expression in nonmuscle cells provides an alternative opportunity to distinguish the functional roles of the two α_{1S} forms. Injection of cRNAs encoding $\alpha_{1S\Delta C}$ plus the muscle-associated β_{1b}, $\alpha_2\delta$, and γ subunits into *Xenopus* oocytes was recently found to give rise to robust DHP-sensitive L-type currents, whereas injection of full-length α_{1S} cDNA gave little or no current (Ren and Hall, 1997). While these results suggest a difference in channel function for α_{1S} and $\alpha_{1S\Delta C}$, they leave open the possibility that full-length α_{1S} simply expresses poorly in oocytes, but conducts Ca^{2+} just as well as $\alpha_{1S\Delta C}$. Moreover, measurements of ionic current alone cannot address the crucial question of whether α_{1S} and $\alpha_{1S\Delta C}$ function differently as voltage sensors.

To study the current-carrying and voltage-sensing capabilities of the two size forms of α_{1S} in parallel, we expressed α_{1S} and $\alpha_{1S\Delta C}$ with the β_1, $\alpha_2\delta$, and γ auxiliary subunits in *Xenopus* oocytes. We examined the β_{1a} and β_{1b} splice variants, both of which are expressed in muscle tissue (Hofmann et al., 1994; Ren and Hall, 1997), because of a previous report that the less-abundant β_{1b} variant was critical for forming channels capable of conducting Ba^{2+} current (Ren and Hall, 1997). The cut-open oocyte voltage clamp technique (Stefani and Bezanilla, 1998) was used to record ionic currents (in 10 mM Ba^{2+}) and gating charge movement (in 2 mM Co^{2+}) in parallel. We found that both size forms of the α_{1S} subunit supported gating charge movements in 2 mM Co^{2+} when expressed with auxiliary subunits in oocytes, even though only the truncated form conducted appreciable L-type currents in 10 mM Ba^{2+}. This result was independent of whether the β_{1a} or β_{1b} splice variant was used. We conclude that, while α_{1S} and $\alpha_{1S\Delta C}$ function almost identically as voltage sensors, $\alpha_{1S\Delta C}$ is the form specialized to carry L-type current, while α_{1S} appears to be somehow inhibited from passing substantial ionic current.

METHODS

The rabbit α_{1S}, rat brain β_{1b}, rabbit $\alpha_2\delta$, and rabbit γ Ca^{2+} channel cDNAs were obtained in the pKCRH, pBluescript, pcDNA3, and pcD-x vectors, respectively, as a gift from Dr. Kevin Campbell (University of Iowa, Iowa City, IA). The rabbit β_{1a} subunit was obtained in the pNKS2 vector as a gift from Dr. Bernhard Flucher (University of Innsbruck, Innsbruck, Austria). α_{1S} and γ were subcloned into the pGEMHE oocyte expression vector (gift of Dr. Emily Liman, Harvard University) at the HindIII and BamHI polylinker sites, respectively. β_{1b} was subcloned into pGEMHE between the SacII and HindIII sites, while $\alpha_2\delta$ and β_{1a} were left in pCDNA3 and pNKS2, respectively. $\alpha_{1S\Delta C}$-pGEMHE was made from α_{1S}-pGEMHE using the Clontech Transformer site-directed mutagenesis kit (CLONTECH Laboratories, Inc.). The mutagenic primer caused a loop-out deletion of base pairs 5320–5844 (amino acids 1698–1893) of the rabbit α_{1S} sequence, while the selection primer mutated the MfeI site at position 2788 of the pGEMHE sequence to a unique NdeI site. For in vitro synthesis of RNA, the plasmids containing the Ca^{2+} channel subunits were linearized using the following restriction enzymes: Sse8387I for α_{1S} and $\alpha_{1S\Delta C}$, XbaI for β_{1a}, NotI for β_{1b}, PvuII for $\alpha_2\delta$, and NheI for γ. Capped cRNA was synthesized using the mMessage mMachine T7 kit (for α_{1S}, $\alpha_{1S\Delta C}$, β_{1b}, $\alpha_2\delta$, and γ) or SP6 kit (for β_{1a}; Ambion Corp.) and extracted using the RNAid purification kit (Bio101).

Stage V and VI oocytes were harvested from egg-bearing female *Xenopus laevis* frogs under anesthesia with 3-aminobenzoic acid ethyl ester (1 mg ml^{-1} in a cold water bath for 25 min; Sigma-Aldrich), in accordance with the guidelines of the Subcommittee on Research Animal Care at the Massachusetts General Hospital. Oocytes were removed into Ca^{2+}-free OR-2 solution containing (mM): 82.5 NaCl, 2.5 KCl, 1 $MgCl_2$, and 5 HEPES, pH 7.6. The egg sacs were manually torn open using forceps, and the oocytes were incubated in OR-2 containing 2 mg ml^{-1} collagenase (GIBCO BRL) for 2.5 h in a room temperature shaker (60 rpm) to remove the follicular membrane. The oocytes were then washed four times in OR-2 solution and transferred for storage to ND-96 solution containing (mM): 96 NaCl, 2 KCl, 1.8 $CaCl_2$, 1 $MgCl_2$, 2.5 pyruvate, 5 HEPES, and 50 μg ml^{-1} gentamicin (GIBCO BRL), pH 7.6. Oocytes were injected with 50–100 nl of a 1:1:1:1 mixture of α_{1S} (or $\alpha_{1S\Delta C}$), β_{1a} (or β_{1b}), $\alpha_2\delta$, and γ cRNA using injection pipettes pulled from thin-wall capillary glass (World Precision Instruments) and were stored at 18°C for 5–7 d before recording.

Oocytes were voltage clamped in the cut-open configuration, with active clamp of the upper and guard compartments, using an oocyte clamp (CA-1B; Dagan Corp.) under control of a custom stimulation/recording program written in AxoBASIC and running on an IBM-compatible computer. Voltage-sensing electrodes, fabricated from borosilicate capillary glass (1.65-mm outer diameter; VWR Scientific) using a multi-stage puller (Sutter Instrument Co.), were filled with 3 M KCl and had resistances of 0.2–1 MΩ. The leads of the amplifier headstage, attached to Ag/AgCl pellets in plastic wells containing 2 M NaCl solution, were connected to the upper, guard, and lower oocyte compartments using glass agar bridges containing 110 mM Na-methanesulfonic acid and 10 mM HEPES, in 3% agarose, pH 7.0, and threaded with a platinum wire. Current traces, evoked by depolarizing test pulses from a holding potential of −90 mV, were corrected for linear leak and capacity currents (minimized by the analog compensation of the amplifier) by addition of control currents evoked by hyperpolarizing pulses of equal amplitude from the holding potential (P/−1 protocol). Since the charge movement was not noticeably altered by changing the holding potential to −110 or −120 mV (data not shown), we judged our leak subtraction protocol to be sufficient to selectively subtract linear components. Signals were filtered at 1 kHz and sampled at 20 kHz (for gating currents) or 2 kHz (for ionic currents). Analysis and curve fitting was performed using a combination of custom AxoBASIC routines and SigmaPlot (Jandel Scientific). Student's *t* test was used to make pairwise comparisons between sets of data (*P* values are reported in the text; $P = 0.05$ was taken as the limit of statistical significance).

Solutions for recording Ba^{2+} currents and Ca^{2+} channel gating currents were prepared following Olcese et al. (1996) and Stefani and Bezanilla (1998) and were Cl^- free to avoid contamination with oocyte Cl^- currents (including Ba^{2+}-activated Cl^- currents). For gating current measurements, the external solution (applied in the external and guard compartments) contained (mM): 2 $Co(OH)_2$, 96 NaOH, and 10 HEPES, adjusted to pH 7.0 with methanesulfonic acid. For ionic current measurements, the external solution contained 10 mM $Ba(OH)_2$ instead of 2 mM

$Co(OH)_2$, but was otherwise identical. The lower chamber in contact with the part of the oocyte permeabilized with 0.1% saponin (Sigma-Aldrich) contained 110 mM potassium glutamate and 10 mM HEPES, adjusted to pH 7.0 with NaOH. To avoid possible contamination with nonlinear charge movement related to the oocyte Na^+–K^+ pump (Neely et al., 1993; Olcese et al., 1996; Stefani and Bezanilla, 1998), 0.1 mM ouabain (Sigma-Aldrich) was present in all external solutions.

RESULTS

Oocytes injected with either α_{1S} or $\alpha_{1S\Delta C}$ plus the auxiliary subunit cRNAs showed transient currents at the beginning and end of short depolarizing pulses, while uninjected oocytes and oocytes injected with auxiliary subunit cRNAs alone lacked these currents (Fig. 1 A). These transient currents had the properties expected of gating currents arising from the movement of charged elements in the ion channel protein: (a) they depended on the presence of the pore-forming α subunit (Fig. 1 A); (b) they always followed the direction of the voltage step (A); (c) the integral of the current at the onset of a voltage step (Q_{on}) matched the integral of the current at the offset of the step (Q_{off}) (B); and (d) Q_{on} and Q_{off} approached limiting values at both positive and negative potentials, with a voltage dependence that followed a Boltzmann distribution (C).

Fig. 2, which compares the magnitude and voltage dependence of the charge movement measured in oocytes expressing α_{1S} and $\alpha_{1S\Delta C}$, shows that both constructs were clearly expressed abundantly at the surface membrane regardless of which β_1 subunit isoform was coexpressed. Q_{off} was used for the comparison instead of Q_{on} because of the faster kinetics (and hence greater single-to-noise ratio at small test depolarizations) of the OFF response. The maximum Q_{off} appeared larger in oocytes expressing $\alpha_{1S\Delta C}$ than in oocytes expressing α_{1S} (Fig. 2, A and B). While this effect on $Q_{off,\,max}$ was not statistically significant in the presence of β_{1a} (Fig. 2 A; $P = 0.13$), it was statistically significant in the presence of β_{1b} (B; $P = 0.008$). The normalized Q_{off} versus voltage (Q-V) curves for α_{1S} and $\alpha_{1S\Delta C}$ had roughly the same midpoints and slopes (Fig. 2 C). As has been observed for other voltage-dependent ion channels and for native L-type Ca^{2+} channels in skeletal muscle, the Q-V curve started at significantly more negative potentials and was less steep than the G-V curve for L-type current (Fig. 2 C, ▼). This is consistent with the idea that skeletal muscle Ca^{2+} channels undergo rapid voltage-dependent transitions among several closed conformations before opening, some of which are presumably involved in excitation–contraction coupling (Feldmeyer et al., 1990; Ma et al., 1996).

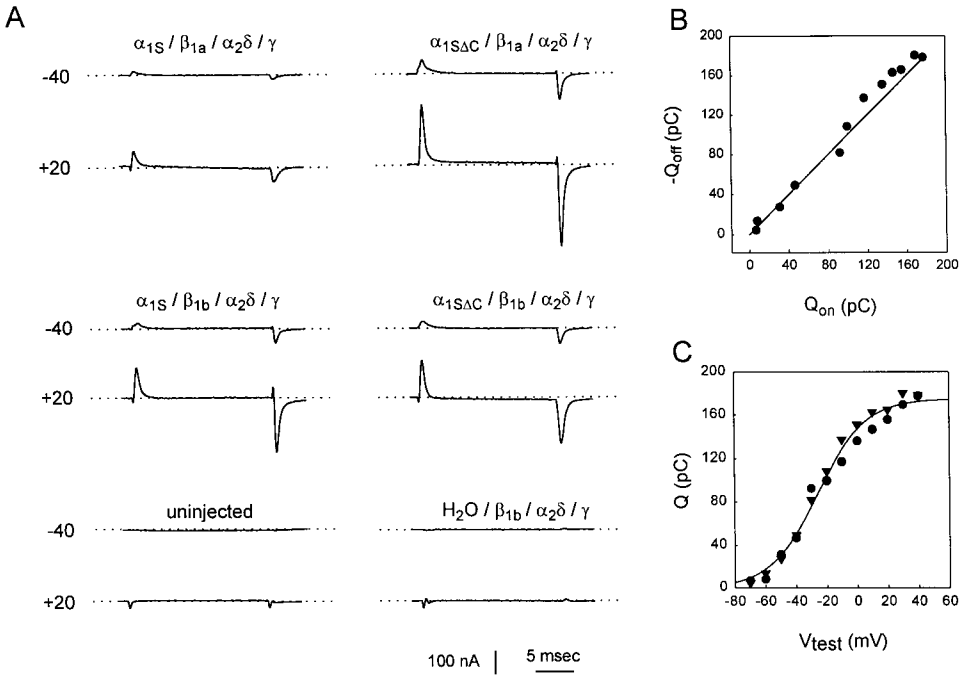

Figure 1. Gating currents from oocytes expressing the truncated and full-length forms of the rabbit skeletal muscle L-type Ca^{2+} channel α_1 subunit ($\alpha_{1S\Delta C}$ and α_{1S}). (A) Voltage-clamp traces recorded in six oocytes during 20-ms depolarizing steps to the values shown on the left from a holding potential of −90 mV. The combination of cRNAs injected is shown above each set of traces. Each trace is the average of four responses filtered at 1 kHz and sampled at 20 kHz. The dotted lines represent zero current. (B) Q_{on} vs. $-Q_{off}$ plot for the $\alpha_{1S\Delta C}$, β_{1b}-injected oocyte from A, middle right, shows charge conservation. A straight line with a slope of 1 is shown as a reference. Values of Q_{on} and Q_{off} were obtained by integrating the gating currents during and after the pulse. 10 datum points (0.5 ms) near the end of the pulse were used to define the baseline for Q_{on}, while 10 datum points near the end of the trace (3–5 ms after the end of the pulse) were used to define the baseline for Q_{off}. Q_{on} was integrated throughout the pulse to allow slow components of charge movement to be included. Q_{off} did not have prominent slow components and was integrated over the first ~3 ms after the pulse. A number of cells showed small, slow tail currents at depolarized potentials (see +20 mV traces in A, top right and middle left) that were excluded from Q_{off} by baseline subtraction. (C) Q_{on} (●) and Q_{off} (▼) versus voltage for the same oocyte were fitted by Boltzmann distributions of the form: $Q\text{-}V = Q_{max}/\{1 + \exp[-(V - V_{1/2Q})/k_Q]\}$, where Q_{max} is the maximal charge moved at depolarized voltages, $V_{1/2Q}$ is the voltage at which charge movement is half maximal, and k_Q describes the steepness of the distribution. The solid line shows the average of the Q_{on} and Q_{off} fits: Q_{max} = 175 pC, $V_{1/2Q} = -25.9$ mV, and $k_Q = 15.6$ mV.

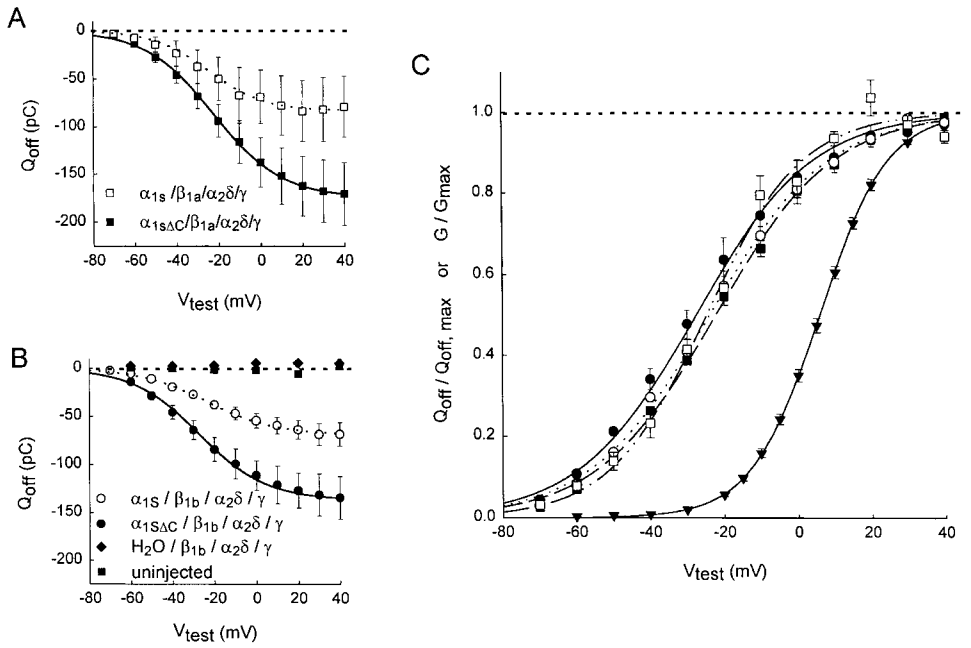

Figure 2. The magnitude and voltage dependence of charge movement in oocytes expressing $\alpha_{1S\Delta C}$ and α_{1S}. (A) Q_{off} versus voltage from five oocytes expressing α_{1S}, β_{1a}, $\alpha_2\delta$, and γ (□) and 12 oocytes expressing $\alpha_{1S\Delta C}$, β_{1a}, $\alpha_2\delta$, and γ (■). The solid and dashed lines through the data points show the mean Boltzmann fits to the data from individual cells (fitted as described in Fig. 1). α_{1S}/β_{1a}/$\alpha_2\delta$/γ: $Q_{off, max} = -82.9 \pm 32.8$ pC, $V_{1/2Q} = -24.7 \pm 2.2$ mV, $k_Q = 13.1 \pm 1.0$ mV, $n = 5$; $\alpha_{1S\Delta C}$/β_{1a}/$\alpha_2\delta$/γ: $Q_{off, max} = -175 \pm 34.0$ pC, $V_{1/2Q} = -22.2 \pm 0.8$ mV, $k_Q = 16.1 \pm 0.3$ mV, $n = 12$. The differences in $Q_{off, max}$ between these two data sets are not statistically significant ($P = 0.13$; see text). (B) Q_{off} versus voltage from nine oocytes expressing α_{1S}, β_{1b}, $\alpha_2\delta$, and γ (○), eight oocytes expressing $\alpha_{1S\Delta C}$, β_{1b}, $\alpha_2\delta$, and γ (●), six oocytes expressing the auxiliary subunits alone (◆), and eight uninjected oocytes (■). Error bars correspond to the standard error of the mean and are smaller than the symbol when not visible. Gating currents were recorded in 2 mM extracellular Co^{2+}, and Q_{off} was calculated as described in Fig. 1. The solid and dashed lines through the symbols are mean Boltzmann fits, as above. α_{1S}/β_{1b}/$\alpha_2\delta$/γ: $Q_{off, max} = -69.0 \pm 11.0$ pC, $V_{1/2Q} = -23.9 \pm 1.3$ mV, $k_Q = 16.2 \pm 0.5$ mV, $n = 9$; $\alpha_{1S\Delta C}$/β_{1b}/$\alpha_2\delta$/γ: $Q_{off, max} = -137 \pm 20.1$ pC, $V_{1/2Q} = -27.5 \pm 3.2$ mV, $k_Q = 15.9 \pm 1.4$ mV, $n = 8$. The differences in $Q_{off, max}$ between these two data sets are statistically significant ($P = 0.008$; see text). (C) Normalized Q_{off} versus voltage (Q-V) curves for oocytes expressing α_{1S} (open symbols) and $\alpha_{1S\Delta C}$ (filled symbols) with β_{1a}, $\alpha_2\delta$, and γ (squares) or β_{1b}, $\alpha_2\delta$, and γ (circles). The Q-V curves are compared with the mean G-V curve measured in 10 mM Ba^{2+} solution for oocytes expressing $\alpha_{1S\Delta C}$, β_{1b}, $\alpha_2\delta$, and γ (▼). To obtain the Q-V curves, data from individual oocytes were fitted by Boltzmann distributions as described above and normalized by $Q_{off, max}$. To obtain the G-V curve, inward L-type currents were evoked by 300-ms depolarizations in 10 mM extracellular Ba^{2+}, filtered at 1 kHz, sampled at 2 kHz, and measured at the end of the pulse. For eight individual oocytes, the I-V curves so obtained were fit to the function: $I\text{-}V = G_{max}(V - E_{rev})/\{1 + \exp[-(V - V_{1/2G})/k_G]\}$, where G_{max} is the maximal conductance attained, E_{rev} is the current reversal potential, $V_{1/2G}$ is the half-activation potential, and k_G describes the steepness of activation. In the fitting procedure, G_{max}, E_{rev}, $V_{1/2G}$, and k_G were all allowed to be free parameters. Normalized G-V curves were then obtained by dividing each I-V curve by $G_{max}(V - E_{rev})$. The lines in C show the average normalized Boltzmann distributions fit to the Q-V and G-V relations measured in individual cells. The fitted parameters for the Q-V curves are given for A and B, above. For the G-V curve: $G_{max} = 3.4 \pm 0.3$ μS, $V_{1/2G} = 5.9 \pm 0.6$ mV, and $k_G = 9.4 \pm 0.2$ mV.

To compare directly the voltage-sensing and current-carrying properties of α_{1S} and $\alpha_{1S\Delta C}$, we measured both ionic and gating currents in individual oocytes expressing these constructs (Fig. 3). In these experiments, ionic currents were measured in the presence of 10 mM Ba^{2+}, the extracellular Ba^{2+} was then replaced with 2 mM Co^{2+} using a manual pipet, and gating charge movements were measured (see Fig. 3, legend). For these experiments, Q_{on} was measured instead of Q_{off}, despite the lower signal-to-noise ratio of the ON response, to avoid the possibility of contamination by small Ba^{2+} tail currents remaining after the solution exchange. These experiments confirmed that the full-length form of the channel conducts Ba^{2+} current very poorly compared with the truncated form (Ren and Hall, 1997), but that injecting cRNA coding for either full-length or truncated α_{1S} resulted in large voltage-driven gating charge movements not found in uninjected eggs. Moreover, this difference was observed whether β_{1a} (Fig. 3, A and B) or β_{1b} (C and D) cRNA was coinjected. The maximal amplitude of the gating currents measured in each egg was comparable with that of the largest ionic current, consistent with the idea that channel expression was high but the channel open probability was low. Indeed, while the ionic currents, even those carried by $\alpha_{1S\Delta C}$, were small compared with those measured for other cloned Ca^{2+} channels expressed in oocytes, the gating currents were as large as or larger than those of other Ca^{2+} channels (Neely et al., 1993; Olcese et al., 1996). This suggests that oocyte expression of the skeletal muscle Ca^{2+} channels is considerably more robust than has been previously believed. Oocytes injected with cRNA coding for the auxiliary subunits alone had DHP-insensitive inward Ba^{2+} currents comparable in size with the L-type current, but with rapid kinetics, presumably carried by an endogenous Ca^{2+} channel (Fig. 3 E, top). These oocytes did not have measurable gating currents (Fig. 3 E, bot-

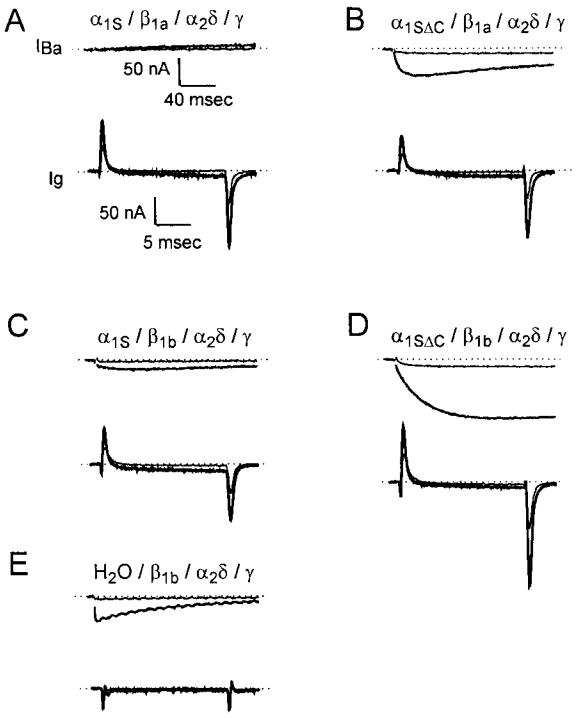

Figure 3. Ionic and gating currents recorded in the same cell for oocytes expressing α_{1S} plus auxiliary subunits, $\alpha_{1S\Delta C}$ plus auxiliary subunits, or auxiliary subunits alone. For each oocyte, inward ionic currents were recorded in 10 mM Ba^{2+} solution. The Ba^{2+} solution was replaced by 2 mM Co^{2+} solution (applied in the bath using a Pasteur pipet), and then gating currents were recorded after capacitance compensation. In A–E, the ionic currents evoked by test pulses to −40 and +20 mV from the holding potential of −90 mV are shown on a slow time scale (top, average of two traces in each case), and the gating currents evoked by test pulses to the same voltages are shown on a much faster time scale (bottom, average of four traces). The lighter traces show the responses at −40 mV, and the darker traces show the responses at +20 mV. Ionic currents were evoked by 300-ms depolarizations, filtered at 1 kHz and sampled at 2 kHz, and are presented with the residual capacitance transients blanked. Gating currents were evoked by 20-ms depolarizations, filtered at 1 kHz and sampled at 20 kHz.

tom), suggesting that the endogenous channel had a much smaller ratio of gating to ionic current than the skeletal muscle channel. Based on its kinetic properties, we judged the small ionic current seen in oocytes injected with cRNA coding for full-length α_{1S} to be mostly, though not completely, endogenous in origin (a conclusion confirmed by separate experiments in which 5 μM nimodipine was found to block <10% of the current expressed in these cells; data not shown). These currents were consistently smaller than the endogenous current observed in oocytes injected with the auxiliary subunit cRNAs alone, most likely because of competition between α_{1S} subunits and endogenous Ca^{2+} channel subunits for the auxiliary subunits.

Comparison of the mean Q_{on}-V and I-V curves measured in oocytes expressing $\alpha_{1S\Delta C}$ and α_{1S} with either the β_{1a} subunit (Fig. 4, A and B) or the β_{1b} subunit (C and D) emphasizes that while the full-length and truncated subunits are comparable voltage sensors, the truncated version is a much better conductor of ionic current. We quantified this functional distinction by calculating the ratio of maximum ionic current to maximum charge movement ($I_{max}/Q_{on,\,max}$) for each oocyte (Fig. 4 E). $I_{max}/Q_{on,\,max}$ was sixfold greater for oocytes expressing $\alpha_{1S\Delta C}$ than for oocytes expressing α_{1S} when either the β_{1a} or the β_{1b} subunit was used; a difference that was highly statistically significant in each case ($P = 4.8 \times 10^{-6}$ and 6.2×10^{-5}, respectively). This difference is a conservative estimate, since at least 90% of the current observed in α_{1S}-injected oocytes was conducted by a DHP-insensitive α subunit, as mentioned above (data not shown). $I_{max}/Q_{on,\,max}$ was smaller for channels containing β_{1a} than for channels containing β_{1b}, reflecting both the somewhat smaller ionic currents and larger gating currents observed, on average, when β_{1a} was injected. As was also seen in the separate experiments of Fig. 2, truncation of the α_{1S} increased the size of gating currents significantly in the presence of the β_{1b} subunit ($P = 0.02$), but not in the presence of the β_{1a} subunit ($P = 0.63$).

DISCUSSION

The primary goal of this study was to determine whether the different magnitudes of L-type Ba^{2+} current observed previously when the full-length α_{1S} and truncated $\alpha_{1S\Delta C}$ subunits were expressed in *Xenopus* oocytes (Ren and Hall, 1997) represents a function specialization of these two size forms of the skeletal muscle L-type Ca^{2+} channel. Using the cut-open oocyte voltage clamp method, we measured large transient currents from oocytes expressing α_{1S} or $\alpha_{1S\Delta C}$ with the β_1 (β_{1a} or β_{1b}), $\alpha_2\delta$, and γ subunits that represented gating charge movements in the α_1 subunit molecule, demonstrating that both size forms of the channel are expressed in oocytes and constitute working voltage sensors. The range and steepness of the voltage dependence of the charge movement mediated by α_{1S} and $\alpha_{1S\Delta C}$ were essentially the same, independent of which β1 subunit was coexpressed. The maximum amount of charge moved at depolarized voltages, Q_{max}, tended to be larger for $\alpha_{1S\Delta C}$ than for α_{1S}. However, this difference in Q_{max} was statistically significant (both $Q_{on,\,max}$ and $Q_{off,\,max}$) only when the β_{1b} subunit, rather than the β_{1a} subunit, was coexpressed. Measurements of both charge movement and ionic current from the same oocyte showed that: (a) oocytes expressing the truncated subunit plus auxiliary subunits supported both charge movements and L-type Ba^{2+} current; (b) oocytes expressing the full-length subunit plus auxiliary subunits had charge movements but very little L-type Ba^{2+} current; and (c) oocytes expressing the

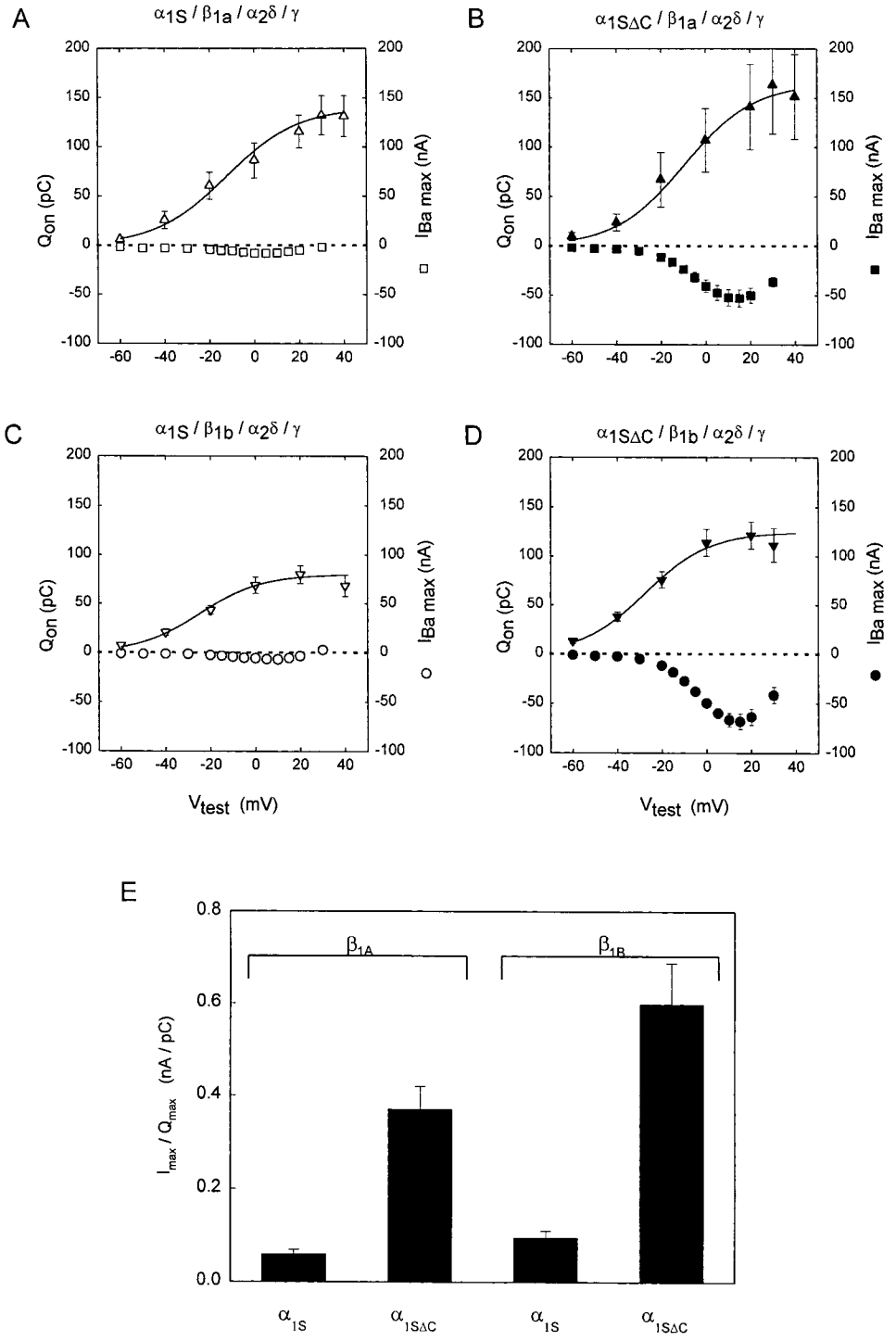

Figure 4. Comparison of ionic current to gating charge movement in oocytes expressing α_{1S} or $\alpha_{1S\Delta C}$ plus the auxiliary subunits. (A–D) Q_{on} versus voltage (left scale) and current versus voltage (right scale) measured in the same oocytes. (A) Data from six cells expressing α_{1S}, β_{1a}, $\alpha_2\delta$, and γ. (B) Data from five cells expressing $\alpha_{1S\Delta C}$, β_{1a}, $\alpha_2\delta$, and γ. (C) Data from 10 cells expressing α_{1S}, β_{1b}, $\alpha_2\delta$, and γ. (D) Data from nine cells expressing $\alpha_{1S\Delta C}$, β_{1b}, $\alpha_2\delta$, and γ. Experiments were performed as in Fig. 3. Q_{on}, measured as described in Fig. 1, was used instead of Q_{off} in these experiments to avoid the possibility of contamination with residual Ba^{2+} tail current. The solid lines are the mean Boltzmann Q-V curves determined as in Fig. 2 for each set of data. In A, $Q_{on,\,max} = 140 \pm 21.6$ pC, $V_{1/2Q} = -12.3 \pm 5.5$ mV, $k_Q = 16.0 \pm 1.7$ mV, $I_{max} = -8.5 \pm 1.1$ nA, and $n = 6$. In B, $Q_{on,\,max} = 165 \pm 47.6$ pC, $V_{1/2Q} = -9.2 \pm 3.3$ mV, $k_Q = 15.6 \pm 2.3$ mV, $I_{max} = -53.0 \pm 8.6$ nA, and $n = 5$. The difference in $Q_{on,\,max}$ between the data in A and in B was not statistically significant ($P = 0.63$). In C, $Q_{on,\,max} = 80.1 \pm 9.6$ pC, $V_{1/2Q} = -24.6 \pm 1.8$ mV, $k_Q = 13.8 \pm 1.4$ mV, $I_{max} = -7.3 \pm 1.1$ nA, and $n = 10$. In D, $Q_{on,\,max} = 125 \pm 16.0$ pC, $V_{1/2Q} = -27.4 \pm 2.6$ mV, $k_Q = 14.4 \pm 1.8$ mV, $I_{max} = -68.8 \pm 7.2$ nA, and $n = 6$. The difference in $Q_{on,\,max}$ between C and D was statistically significant ($P = 0.02$). (*E*) Ratio of maximum Ba^{2+} current (I_{max}) to $Q_{on,\,max}$ in cells expressing $\alpha_{1S\Delta C}$ or α_{1S} plus auxiliary subunits. For each cell, the maximum inward current evoked by a 300-ms depolarization to +10 or +15 mV in 10-mM Ba^{2+} solution was divided by the value of $Q_{on,\,max}$ determined from the Boltzmann fit to the Q_{on} versus voltage relationship. In cells expressing the β_{1a} subunit, $I_{max}/Q_{on,\,max}$ was 0.06 ± 0.01 nA/pC when α_{1S} was expressed and 0.37 ± 0.05 nA/pC when $\alpha_{1S\Delta C}$ was expressed, a difference which was statistically significant ($P = 4.8 \times 10^{-6}$). In cells expressing the β_{1b} subunit, $I_{max}/Q_{on,\,max}$ was 0.10 ± 0.01 nA/pC when α_{1S} was expressed and 0.60 ± 0.09 nA/pC when $\alpha_{1S\Delta C}$ was expressed, a difference which was also statistically significant ($P = 6.2 \times 10^{-5}$).

auxiliary subunits alone had neither detectable charge movements nor L-type Ba^{2+} current. The stark differences observed between cells expressing α_{1S} versus $\alpha_{1S\Delta C}$ suggest there was no appreciable COOH-terminal truncation of α_{1S} in the oocyte.

We conclude that the two naturally occurring size forms of the skeletal muscle DHP receptor α subunit are functionally specialized when expressed with the auxiliary subunits found in muscle. α_{1S} and $\alpha_{1S\Delta C}$ are both functional voltage sensors, but $\alpha_{1S\Delta C}$ is a much

more effective Ca^{2+} channel. Only tiny ionic currents were seen when the α_{1S} subunit was coexpressed with either the β_{1a} or β_{1b} subunit (Fig. 4, A and C), and the currents observed when the $\alpha_{1S}/\beta_{1b}/\alpha_2\delta/\gamma$ combination was injected were ~90% insensitive to 5 μM nimodipine (data not shown). This differs from the data of Ren and Hall (1997), who observed what appeared to be L-type current when α_{1S} was expressed with β_{1b}, $\alpha_2\delta$, and γ (although this conclusion was based on current kinetics rather than on dihydropyridine block). We observed robust ionic currents when either β_{1a} or β_{1b} cRNAs were coinjected with $\alpha_{1S\Delta C}$ cRNA, in contrast to the original report of a requirement for β_{1b} (Ren and Hall, 1997). Moreover, separate experiments in which 5 μM nimodipine was applied to oocytes expressing the $\alpha_{1S\Delta C}/\beta_{1a}/\alpha_2\delta/\gamma$ combination confirmed that the inward current seen in this case was 80–90% L-type (data not shown). Our results therefore support the hypothesis that the predominant form of native DHP receptors in skeletal muscle, those containing $\alpha_{1S\Delta C}$ and β_{1a}, can function both as voltage sensors and as L-type calcium channels. Given the strong similarity of the kinetics and voltage dependence of the ionic and gating currents measured here in oocytes to those measured previously in mammalian muscle cells (Dulhunty and Gage, 1983; Simon and Beam, 1985; Lamb, 1987; Delbono, 1992; Garcia et al., 1992), we believe that the functional differences we observed for α_{1S} and $\alpha_{1S\Delta C}$ in oocytes are likely to occur in native DHP receptors. Nevertheless, experimental confirmation of the distinct functional roles of the α_{1S} and $\alpha_{1S\Delta C}$ subunits must ultimately be delineated in native cells, especially given the mounting evidence from dyspedic myotubes that both functions of the DHP receptor are strongly influenced by interacting ryanodine receptors (Nakai et al., 1996; Avila and Dirksen, 2000). Definitive proof of distinct roles for the two size forms of the α_{1S} subunit may ultimately require the identification and selective inhibition of the enzyme responsible for COOH-terminal truncation.

The mechanism by which the carboxyl terminus modulates the coupling between voltage-dependent gating and channel opening remains unknown. A similar effect has been observed for the cardiac L-type Ca^{2+} channel. Deletion of amino acids 307–472 from the 665-amino acid carboxyl terminus of the α_{1C} subunit increased Ba^{2+} currents four- to sixfold in the oocyte expression system (Wei et al., 1994). The increase in ionic current did not appear to be accompanied by an increase in gating charge, consistent with the notion that the coupling was enhanced, rather than an increase in the number of channels. The confidence in this conclusion is somewhat limited, however, by the fact that charge movements were measured in the presence of large, unblocked inward Ba^{2+} currents. Several motifs important for modulation of Ca^{2+} currents have been identified in the carboxyl tails of α subunits. The carboxyl terminus deletion of α_{1S} studied herein removes several consensus sites for PKC and cAMP-mediated phosphorylation, but leaves intact an EF hand and calmodulin-binding IQ consensus motifs, both of which have been implicated in Ca^{2+}-dependent modulation of inactivation and facilitation of ionic current (Lee et al., 1999; Zühlke et al., 1999). It remains to be determined whether the enhanced coupling of gating charge movement to channel opening we observed in $\alpha_{1S\Delta C}$ is dependent on any of these previously identified modulatory roles of the carboxyl terminus. Our observation that truncation of the α_{1S} subunit significantly increased the magnitude of gating charge movements (an effect not seen with COOH-terminal truncation of α_{1C}) suggests that the COOH terminus of α_{1S} may play a role in channel expression in the membrane as well as in the coupling of gating to pore opening.

Our experiments give the unexpected result that both size forms of the α_{1S} subunit express as well as or better than other cloned Ca^{2+} channel isoforms in *Xenopus* oocytes, as judged by gating current amplitudes (Neely et al., 1993; Olcese et al., 1996). This finding contradicts the common belief that the small ionic currents seen by us and others trying to express α_{1S} in heterologous systems (Perez-Reyes et al., 1989; Nargeot et al., 1992; Johnson et al., 1997) reflect an inability of this channel to express stably outside the muscle environment. On the other hand, the local environment of the triadic junction does enhance the efficacy of DHP receptors to function as Ca^{2+} channels, as shown by a decrease in the ratio of ionic to gating current in dyspedic mice lacking the skeletal muscle isoform of the ryanodine receptor (Nakai et al., 1996). The large gating currents we observed relative to the small ionic currents underscore the idea that the coupling of charge movement to pore opening is poor in DHP receptors (Flockerzi et al., 1986; Ma et al., 1991; Dirksen and Beam, 1995), even for channels containing the truncated α_{1S} subunit. Robust expression of the skeletal muscle L-type Ca^{2+} channel in a heterologous system will be useful in elucidating the functional consequences of muscle-specific modulatory mechanisms, which may include modifications to the channel protein (such as phosphorylation or the COOH-terminal truncation studied here) or interactions with other proteins (such as the auxiliary Ca^{2+} channel subunits or other components of the triad junction). In addition, the ability to record skeletal muscle Ca^{2+} channel gating currents in an expression system lacking the electrically complex features of muscle cells, such as t tubules and additional voltage-gated channels, may allow for unprecedented precision in the study of the channel voltage sensor.

The authors thank B.P. Bean for lending the oocyte clamp and for comments on the manuscript.

This work was supported by the National Institute of Arthritis, Musculoskeletal and Skin Diseases (AR42703 to S.C. Cannon) and the Quan Fellowship to Harvard Medical School (J.A. Morrill).

Submitted: 20 April 2000
Revised: 5 July 2000
Accepted: 18 July 2000

REFERENCES

Adams, B.A., T. Tanabe, A. Mikami, S. Numa, and K.G. Beam. 1990. Intramembrane charge movement restored in dysgenic skeletal muscle by injection of dihydropyridine receptor cDNAs. *Nature*. 346:569–572.

Avila, G., and R.T. Dirksen. 2000. Functional impact of the ryanodine receptor on the skeletal muscle L-type Ca^{2+} channel. *J. Gen. Physiol.* 115:467–480.

Beam, K.G., B.A. Adams, T. Niidome, S. Numa, and T. Tanabe. 1992. Function of a truncated dihydropyridine receptor as both voltage sensor and calcium channel. *Nature*. 360:169–171.

De Jongh, K.S., D.K. Merrick, and W.A. Catterall. 1989. Subunits of purified calcium channels: a 212-kDa form of α_1 and partial amino acid sequence of a phosphorylation site of an independent β subunit. *Proc. Natl. Acad. Sci. USA.* 86:8585–8589.

De Jongh, K., C. Warner, A.A. Colvin, and W.A. Catterall. 1991. Characterization of the two size forms of the α_1 subunit of skeletal muscle L-type calcium channels. *Proc. Natl. Acad. Sci. USA.* 88: 10778–10782.

Delbono, O. 1992. Calcium current activation and charge movement in denervated mammalian skeletal muscle fibres. *J. Physiol.* 451:187–203.

Dirksen, R.T., and K.G. Beam. 1995. Single calcium channel behavior in native skeletal muscle. *J. Gen. Physiol.* 105:227–247.

Dulhunty, A.F., and P.W. Gage. 1983. Asymmetrical charge movement in slow- and fast-twitch mammalian muscle fibres in normal and paraplegic rats. *J. Physiol.* 341:213–231.

Feldmeyer, D., W. Melzer, B. Pohl, and P. Zollner. 1990. Fast gating kinetics of the slow Ca^{2+} current in cut skeletal muscle fibres of the frog. *J. Physiol.* 425:347–367.

Flockerzi, V., H.-J. Oeken, F. Hofmann, D. Pelzer, A. Cavalie, and W. Trautwein. 1986. Purified dihydropyridine-binding site from skeletal muscle t-tubules is a functional calcium channel. *Nature*. 323: 66–68.

Flucher, B.E., B. Neuhuber, and U. Gerster. 1999. The full-length form of the skeletal muscle calcium channel α_{1S} subunit is inserted into triads. *Biophys. J.* 76:A342.

Garcia, J., K. McKinley, S.H. Appel, and E. Stefani. 1992. Ca^{2+} current and charge movement in adult single human skeletal muscle fibres. *J. Physiol.* 454:83–196.

Hofmann, F., M. Biel, and V. Flockerzi. 1994. Molecular basis for Ca^{2+} channel diversity. *Annu. Rev. Neurosci.* 17:399–418.

Johnson, B.D., J.P. Brousal, B.Z. Peterson, P.A. Gallombardo, G.H. Hockerman, Y. Lai, T. Scheuer, and W.A. Catterall. 1997. Modulation of the cloned skeletal muscle L-type Ca^{2+} channel by anchored cAMP-dependent protein kinase. *J. Neurosci.* 17:1243–1255.

Lamb, G.D. 1987. Asymmetric charge movement in polarized and depolarized muscle fibres of the rabbit. *J. Physiol.* 383:349–367.

Lee, A., S.T. Wong, D. Gallagher, B. Lin, D.R. Storm, T. Scheuer, and W.A. Catterall. 1999. Ca^{2+}/calmodulin binds to and modulates P/Q-type calcium channels. *Nature.* 399:155–159.

Ma, J., A. Gonzalez, and R. Chen. 1996. Fast activation of dihydropyridine-sensitive calcium channels of skeletal muscle: multiple pathways of channel gating. *J. Gen. Physiol.* 108:221–232.

Ma, J., C. Mundina-Weilenmann, M.M. Hosey, and E. Ríos. 1991. Dihydropyridine-sensitive skeletal muscle Ca channels in polarized planar bilayers. 1. Kinetics and voltage dependence of gating. *Biophys. J.* 60:890–901.

Melzer, W., A. Hermann-Frank, and H.C. Lüttgau. 1995. The role of Ca^{2+} ions in excitation–contraction coupling of skeletal muscle fibres. *Biochim. Biophys. Acta.* 1241:59–116.

Nakai, J., R.T. Dirksen, H.T. Nguyen, I.N. Pessah, K.G. Beam, and P.D. Allen. 1996. Enhanced dihydropyridine receptor channel activity in the presence of ryanodine receptor. *Nature*. 380:72–75.

Nargeot, J., N. Dascal, and H.A. Lester. 1992. Heterologous expression of calcium channels. *J. Membr. Biol.* 126:97–108.

Neely, A., X. Wei, R. Olcese, L. Birnbaumer, and E. Stefani. 1993. Potentiation by the β subunit of the ratio of the ionic current to the charge movement in the cardiac calcium channel. *Science.* 262:575–578.

Olcese, R., A. Neely, N. Qin, X. Wei, L. Birnbaumer, and E. Stefani. 1996. Coupling between charge movement and pore opening in vertebrate neuronal α_{1E} calcium channels *J. Physiol.* 497:675–686.

Perez-Reyes, E., H.S. Kim, A.E. Lacerda, W. Horne, X. Wei, D. Rampe, K.P. Campbell, A.M. Brown, and L. Birnbaumer. 1989. Induction of calcium currents by the expression of the α_1-subunit of the dihydropyridine receptor from skeletal muscle. *Nature*. 340:233–236.

Ren, D., and L.M. Hall. 1997. Functional expression and characterization of skeletal muscle dihydropyridine receptors in *Xenopus* oocytes. *J. Biol. Chem.* 272:22393–22396.

Ríos, E., and G. Brum. 1987. Involvement of dihydropyridine receptors in excitation–contraction coupling in skeletal muscle. *Nature.* 325:717–720.

Schwartz, L.M., E.W. McCleskey, and W. Almers. 1985. Dihydropyridine receptors in muscle are voltage-dependent but most are not functional calcium channels. *Nature.* 314:747–751.

Simon, B.J., and K.G. Beam. 1985. Slow charge movement in mammalian skeletal muscle. *J. Gen. Physiol.* 85:1–19.

Stefani, E., and F. Bezanilla. 1998. Cut-open oocyte voltage clamp technique. *Methods Enzymol.* 293:300–318.

Tanabe, T., K.G. Beam, J.A. Powell, and S. Numa. 1988. Restoration of excitation–contraction coupling and slow calcium current in dysgenic muscle by dihydropyridine receptor complementary DNA. *Nature.* 336: 134–139.

Wei, X., A. Neely, A.E. Lacerda, R. Olcese, E. Stefani, E. Perez-Reyes, and L. Birnbaumer. 1994. Modification of Ca^{2+} channel activity by deletions at the carboxyl terminus of the cardiac α_1 subunit. *J. Biol. Chem.* 269:1635–1640.

Zühlke, R.D., G.S. Pitt, K. Deisseroth, R. W Tsien, and H. Reuter. 1999. Calmodulin supports both inactivation and facilitation of L-type calcium channels. *Nature*. 399:159–162.